1. INTRODUCTION

The principles of artery-specific SPECT/CT partition model (MIRD) macrodosimetry were introduced in 2011 (*1*). The reader is encouraged to read this text in conjunction with online resources and worked examples freely downloadable from our website to aid in understanding of this dosimetric technique (*2*).

2. ^{99m}TC-MAA SPECT/CT SCAN PROTOCOL

Gamma imaging was performed within 60 minutes of ^{99m}Tc-MAA injection using a hybrid SPECT/CT scanner (Philips Precedence) with a dual-head gamma camera integrated with a 16-slice multi-detector CT.

Liver-to-lung shunt scintigraphy was performed by planar imaging of the lungs and abdomen in anterior and posterior positions. Each planar image was acquired over 120 seconds using a 256 x 256 matrix. Quantification of planar liver-to-lung shunt was performed without attenuation or scatter correction. Planar regions-of-interest (ROIs) were contoured over the liver, right and left lungs in anterior and posterior views to obtain respective geometric means. Regions of liver not injected with ^{99m}Tc-MAA are excluded from ROI analysis. For example, for unilobar right lobe tumors, selective right lobe ^{99m}Tc-MAA injection spares the left lobe; hence the liver ROI should include only the targeted right lobe territory. The planar liver-to-lung shunt fraction is calculated according to standard technique (*3*).

For SPECT acquisition, 128 frames (20 seconds per frame, angle step of 3 degrees) were acquired over 360 degrees with a 128 x 128 matrix using a low-energy high-resolution (LEHR) collimator, photopeak 140 ± 10% keV. Unenhanced CT was performed with exposure parameters at 120kV, tube current 50mAs/slice and 5mm slice thickness. CT is used for anatomical correlation as well as SPECT attenuation and scatter correction. SPECT and CT data were processed and fused using Philips Extended Brilliance Workspace Nuclear Medicine (version 1.0) software.

3. ^{99m}Tc-MAA SPECT/CT ANALYSIS

^{99m}Tc-MAA SPECT/CT Analysis of Planning Target Volumes

In the context of ^{90}Y radioembolization, the 'planning target volume' refers to the intended portion of the liver for intra-arterial radiomicrosphere treatment, a term adapted from external beam radiation therapy (EBRT) (*4*). This may involve any combination of sub-segments, segments, lobes or the whole liver. The margins of planning target volumes are delineated by catheter-directed CT hepatic angiography (CTHA). Each planning target volume represents the perfused territory specific to the artery injected with ^{99m}Tc-MAA and its corresponding catheter position.

SPECT/CT is a dual-modality functional (SPECT) and anatomical (CT) imaging modality using a hybrid gamma camera with integrated multi-detector CT. The CT component improves SPECT qualitative and quantitative accuracy by enabling

anatomical localization, attenuation and scatter correction that is superior to that afforded under planar scintigraphy. Phantom studies have shown that ^{99m}Tc-MAA SPECT/CT volume measurements are accurate and reproducible (*5*). By visual co-registration of the ^{99m}Tc-MAA SPECT/CT with its corresponding transaxial catheter-directed CTHA image slice, artery-specific ROIs that contour the planning target volumes are drawn onto the transaxial SPECT/CT slices. ^{99m}Tc-MAA SPECT/CT ROI delineation of territorial boundaries between two adjacent planning target volumes is achieved by visual approximation of perfusion margins as depicted by catheter-directed CTHA. . ^{99m}Tc-MAA SPECT/CT ROIs are interpolated into artery-specific volumes-of-interest (VOIs), each representing a planning target volume with the 'perfused territory SPECT/CT VOI (mm^3)' and its corresponding 'perfused territory SPECT/CT VOI counts'. Non-tumorous liver without ^{99m}Tc-MAA activity (i.e. 'non-implanted non-tumorous liver') should be excluded from dosimetric analysis e.g. liver cysts, post-ablation cavities.

^{99m}Tc-MAA SPECT/CT Analysis of Tumor

Hepatic intra-arterial ^{99m}Tc-MAA may be regarded as a surrogate for ^{90}Y resin microspheres, and ^{99m}Tc-MAA scintigraphy tomographically assesses the outcome of microparticle release-flow-implantation within planning target volumes (*6-8*). In essence, ^{99m}Tc-MAA scintigraphy may be considered a 'simulation study' for ^{90}Y resin microsphere predictive dosimetry. Each ^{99m}Tc-MAA simulation is specific for its artery, catheter tip position, catheter type, injection rate and regional blood flow environment. Any changes to these factors may potentially invalidate the ^{99m}Tc-MAA simulation with

unpredictable effects on the intended dosimetry (see section on 'Limitations and potential sources of error').

During mapping hepatic angiography, ^{99m}Tc-MAA (Technescan LyoMAA®; 111-185MBq in 3ml; ~0.9x10^6 particles) is slowly hand-injected non-selectively (whole-liver), selectively (lobar) or super-selectively (segmental or sub-segmental) depending on patient-specific circumstances (*9*). For example, a patient with bilobar multifocal HCC may be favored for a single non-selective ^{99m}Tc-MAA injection at a proximal main artery (e.g. proper hepatic artery), whereas a patient with unilobar multifocal HCC may benefit from selective ^{99m}Tc-MAA injection at a lobar artery (e.g. right or left hepatic artery).

Assessment of tumor microparticle implantation within each planning target volume should be based primarily on ^{99m}Tc-MAA SPECT/CT, carefully correlated to diagnostic sectional imaging or catheter-directed CTHA (*5,8*). The threshold SPECT intensity for assessing ^{99m}Tc-MAA biodistribution in each planning target volume should most closely approximate tumor margins as seen on diagnostic sectional imaging or catheter-directed CTHA. Imaging discordance between ^{99m}Tc-MAA SPECT/CT versus diagnostic sectional imaging or catheter-directed CTHA are resolved in favor of ^{99m}Tc-MAA SPECT/CT, as it more accurately represents hepatic intra-arterial microparticle biodistribution (*5,8*).

For dosimetric purposes, a 'scintigraphic tumor ROI' is defined as a focal area of ^{99m}Tc-MAA activity with a corresponding lesion seen on either diagnostic sectional

imaging or catheter-directed CTHA. Such a lesion represents an area of tumoral ^{99m}Tc-MAA implantation. Occasionally, focal ^{99m}Tc-MAA activity may occur without any visually detectable corresponding lesion on sectional imaging. The clinical significance of such lesions is uncertain. At present, we recommend these lesions to be regarded as non-tumorous liver for dosimetry.

Scintigraphic tumor ROIs are contoured on each transaxial slice of ^{99m}Tc-MAA SPECT/CT for all visually detectable lesions. Necrotic areas within tumors should be excluded from analysis. Within each planning target volume, scintigraphic tumor ROIs are interpolated into discrete tumor VOIs. All tumor VOIs are summed into a single '*implanted tumor SPECT/CT VOI (mm^3)*' and its corresponding '*implanted tumor SPECT/CT counts*', specific to each planning target volume. A ratio of the two derives the '*implanted tumor mean SPECT/CT count density (counts/mm^3)*'.

^{99m}Tc-MAA SPECT/CT Analysis of Non-Tumorous Liver

Within each planning target volume, the '*implanted non-tumorous liver SPECT/CT VOI (mm^3)*' is calculated as the difference between the 'perfused territory SPECT VOI' and its corresponding 'implanted tumor SPECT VOI'. The '*implanted non-tumorous liver SPECT/CT counts*' is similarly calculated. A ratio of the two derives the '*implanted non-tumorous liver mean SPECT/CT count density (counts/*mm^3*)*'. Required variables are summarized in Supplemental Table 1. Items which should be excluded from dosimetric analysis are listed in Supplemental Table 2.

Artery-Specific Mean T/N Ratio Calculation

The tumor-to-normal liver (T/N) ratio is a patient-specific and sometimes lesion-specific measure of the relative difference in microsphere implantation between tumorous and non-tumorous regions due to differences in vascularity (*10-13*). Hepatic intra-arterial ^{99m}Tc-MAA scintigraphy may be used to estimate the mean T/N ratio (*6,8,12-15*).

The '*artery-specific mean T/N ratio*' is calculated as the ratio of each artery-specific '*implanted tumor mean SPECT/CT count density*' to its corresponding '*implanted non-tumorous liver mean SPECT/CT count density*', expressed as a dimensionless number. This takes into account all inter- and intra-lesional variations in T/N ratios within the same planning target volume to derive a SPECT/CT-based, artery-specific mean T/N ratio.

Liver-to-Lung Shunt Correction for a Change in Plan

Intra-tumoral arteriovenous shunting is a feature of neoplastic vasculature which may lead to pulmonary shunting of injected ^{90}Y microspheres (*16*). Significant pulmonary shunting of ^{90}Y microspheres may manifest clinically as radiation pneumonitis, which may be fatal. Hence, determination of the liver-to-lung shunt fraction is essential for safe ^{90}Y radioembolization.

In some patients, the final ^{90}Y radioembolization plan may be different from that first conceived during mapping hepatic angiography and ^{99m}Tc-MAA injection. For example, a patient initially planned for whole-liver ^{90}Y radioembolization (e.g. underwent whole-liver ^{99m}Tc-MAA injection via the proper hepatic artery during mapping hepatic angiography) may instead be more suitable for segmental ^{90}Y radioembolization via super-selective injections. This situation may arise if, after ^{99m}Tc-MAA injection: 1) there is retrospective discovery of extra-hepatic arteries at risk which are deemed uncorrectable or; 2) there are new concerns about liver reserve and greater sparing of non-tumorous liver from radiation injury is desired.

To maintain dosimetric integrity to lungs, the liver-to-lung shunt contributed by the excluded arterial territory should be omitted from the original liver-to-lung shunt. A key assumption is that ^{99m}Tc-MAA liver-to-lung shunt is directly proportional to tumor mass. Hence, the original liver-to-lung shunt should be reduced in proportion to the tumor mass in the omitted arterial territory, in relation to the total tumor mass across all planning target volumes. A dosimetric worksheet capable of such lung shunt corrections can be freely downloaded from our website (*2*).

Final Dosimetric Calculation

Once all required variables are obtained (Supplemental Table 1), partition model (MIRD) macrodosimetry is applied to all planning target volumes to derive the desired artery-specific ^{90}Y activities and predicted mean radiation absorbed dose (Gy)

estimates to tumor, non-tumorous liver and lung compartments, i.e. one partition model per planning target volume. This will yield one or more radiation plans for every patient depending on the number of planning target volumes. Each radiation plan is independent and unique to its artery and ^{99m}Tc-MAA injection position. The total desired ^{90}Y activity (GBq) for a patient is the sum of all desired ^{90}Y activities across all planning target volumes.

4. BREMSSTRAHLUNG SPECT/CT SCAN PROTOCOL

For SPECT acquisition, 128 frames (20 seconds per frame, angle step of 3 degrees) were acquired over 360 degrees with a 128 x 128 matrix using a medium energy general purpose (MEGP) collimator, photopeak at 80 ± 15% keV. Unenhanced CT was performed with exposure parameters at 120kV, tube current 50mAs/slice and 5mm slice thickness. CT was used for anatomical correlation as well as SPECT attenuation and scatter correction. SPECT and CT data were processed and fused using Philips Extended Brilliance Workspace Nuclear Medicine (version 1.0) software.

5. LIMITATIONS AND POTENTIAL SOURCES OF ERROR

^{99m}Tc-MAA as Surrogate for ^{90}Y Resin Microspheres

^{99m}Tc-MAA approximates ^{90}Y resin microspheres in terms of size and density, and may be used for pre-therapy simulation (*8*). However, ^{99m}Tc-MAA is an imperfect

surrogate and its validity is specific to the catheter tip position, catheter type, injection rate and locoregional flow environment. The locoregional flow environment is itself affected by a multitude of factors, such as the patient's cardiovascular status, tumor-specific vascularity, vasospasm, prophylactic coil embolization, the practice of 'flow re-distribution' and dynamic microvascular flow changes induced by progressive irreversible microembolism during radioembolization. In practice, variations to these technical, biophysical and hemodynamic factors are often unavoidable and unpredictable. Significant changes to any of these factors may potentially invalidate the dosimetry. Therefore, pre-therapy microparticle simulation using ^{99m}Tc-MAA cannot mimic the actual ^{90}Y radioembolization exactly and should only be regarded as a close estimate. Where appropriate, adjustments to the dosimetric plan may be made based on the nuclear medicine physician's experience, clinical judgment and overall assessment of patient-specific circumstances.

As ^{99m}Tc-MAA is an imperfect surrogate, pre-therapy dosimetric error is inevitable. In theory, quantification of dosimetric error is possible by comparing the desired radiation absorbed doses predicted by ^{99m}Tc-MAA, to post-radioembolization in-vivo quantification of the final (i.e. true) ^{90}Y microsphere biodistribution, either by bremsstrahlung scintigraphy or ^{90}Y internal pair production PET/CT. In practice however, post-radioembolization in-vivo quantification is problematic due to inherent technical limitations: bremsstrahlung is essentially scatter radiation, while ^{90}Y PET/CT is vulnerable to background 'noise' due to its very low positron fraction. ^{90}Y PET/CT seems more promising of the two, and this is currently under investigation at our institution.

Manual ROI Contouring

At present, technical limitations at our institution require ROI contouring to be performed manually by 'visual co-registration' of ^{99m}Tc-MAA SPECT/CT with catheter-directed CTHA. This process is prone to subjective error. However, one must realize that conventional (planar) partition modeling is also vulnerable to similar issues of subjectivity. At our institution, nuclear medicine trainees undergo dosimetry training under close supervision by experienced seniors to achieve consistency in ROI contouring, thus minimizing inter-individual variation. The trainee compares and quantifies his/her ROI contouring errors against that of an experienced senior colleague, for the same patient. In the future, it is hoped that problems of subjectivity may be overcome by software solutions capable of automated co-registration of catheter-directed CTHA with ^{99m}Tc-MAA SPECT/CT, and SPECT/CT VOI isocontouring.

Overlapping Arterial Territories

Overlapping regions of arterial perfusion between adjacent territorial boundaries may lead to ambiguity to the margins of planning target volumes. At present, our recommendation is to seek 'middle ground' in-between adjacent regions of overlapping perfusion by visual approximation.

^{99m}Tc-MAA SPECT/CT Spatial Resolution

Limitations in ^{99m}Tc-MAA SPECT/CT spatial resolution may cause partial volume effect in small lesions (e.g. <20cm^3) (*17*). Radiotracer foci in close proximity may also result in the coalescence and/or 'spill-in' of adjacent activity. These may lead to errors in ^{99m}Tc-MAA SPECT/CT VOI determination.

SPECT/CT Mis-Registration

Breathing and other patient movements during SPECT acquisition may cause SPECT/CT mis-registration, especially at the liver dome. One must be mindful that the purpose of ROI contouring is to obtain VOI counts of implanted ^{99m}Tc-MAA activity and its corresponding volume. Hence, in regions of SPECT/CT mis-registration, one should be guided more by the extent of ^{99m}Tc-MAA activity on SPECT, rather than CT anatomical contours. Respiratory-gated SPECT/CT may be a possible solution (*18*).

Arterio-Portal Shunting

Tumor invasion into the hepatic portal vein (main or branch) may cause arterio-portal shunting of ^{99m}Tc-MAA into non-tumorous liver. Clinically significant arterio-portal shunting is usually detectable at mapping hepatic angiography. It is important for the extent of arterio-portal shunting into untargeted lobes/segments to be dosimetrically accounted for, because it increases the non-tumorous liver volume exposed to ^{90}Y

microspheres and decreases the mean T/N ratio. The outcome will be less effective ^{90}Y radioembolization and higher liver toxicity due to reduced tumor radiation absorbed doses but increased non-tumorous liver radiation absorbed doses.

In cases of a single injection of ^{99m}Tc-MAA, the extent of arterio-portal shunting into untargeted lobes/segments can be quantified on ^{99m}Tc-MAA SPECT/CT by VOI analysis of ^{99m}Tc-MAA activity shunted in untargeted territories. These territories should be regarded as part of 'non-tumorous liver' in the overall dosimetry. However, if ^{99m}Tc-MAA is injected into multiple arterial territories, the artery-specific arterio-portal shunting becomes difficult to quantify and the overall dosimetry becomes less reliable. In the future, alternating injections of different tracer-labelled microparticles (e.g. ^{99m}Tc, ^{111}In, ^{131}I, etc.) combined with imaging at different time-points may enable quantification of artery-specific arterio-portal shunting across multiple target arteries by means of scintigraphic energy discrimination.

6. OTHER TECHNICAL NOTES

Alternatives to Catheter-Directed CT Hepatic Angiography

Institutions without catheter-directed CTHA may use cone-beam CT, albeit poorer image quality. If no intra-arterial CT is available in the angiography suite, it may be possible to attempt dual-tracer SPECT/CT to delineate multiple territorial boundaries by means of scintigraphic energy discrimination. For example, ^{99m}Tc-MAA may be

injected alternately with indium-111-MAA (^{111}In-MAA) into different targeted arteries, followed by SPECT/CT. In principle, dual-tracer with different-time point SPECT/CT, with energy windows appropriately calibrated for ^{99m}Tc and ^{111}In may delineate planning target volumes to guide ROI contouring and activity quantification.

Liver-to-Lung Shunt Calculation by SPECT/CT

Liver-to-lung shunting is traditionally calculated using ^{99m}Tc-MAA planar scintigraphy. However, planar scintigraphy may over-estimate the true liver-to-lung shunt due to scatter, radiotracer activity 'spill in' at the right lung base from the liver dome and background activity due to free ^{99m}Tc-pertechnetate. ^{99m}Tc-MAA lung SPECT/CT has the potential to provide more accurate liver-to-lung shunt estimates due to tomographical analysis, attenuation and scatter correction, and should be encouraged (*19*).

7. OTHER CLINICAL APPLICATIONS

Predictive dosimetry by artery-specific SPECT/CT partition modeling in combination with selective/super-selective ^{90}Y microsphere injection enables the safe and effective treatment of hypovascular liver tumors by 'radioembolization lobectomy/segmentectomy'. We define 'hypovascular' liver tumors as tumors identified on diagnostic cross-sectional imaging, but do not exhibit angiographic hypervascularity or focal activity on ^{99m}Tc-MAA scintigraphy. Such tumors usually have poor mean T/N ratios (e.g. <1.5). Exemplified by Patient 2, hypovascular liver tumors *can* be treated to a

desired tumoricidal radiation dose, with the *planned intent* to cause controlled collateral radiation injury to non-tumorous liver, where progressive atrophy of the treated lobe/segment is the anticipated post-radioembolization effect. Such high control over the desired tumor response is not possible by the 'body surface area (BSA)' method. In principle, artery-specific SPECT/CT partition modeling allows most liver tumors to be treated by ^{90}Y radioembolization regardless of their angiographic vascularity or T/N ratio, provided adequate sparing of non-tumorous liver can be achieved.

It may be possible expand the use of artery-specific SPECT/CT partition modeling to plan safe and effective ^{90}Y radioembolization for non-liver solid tumors e.g. 'radioembolization nephrectomy' for inoperable renal cancer. In 1964, Blanchard *et al.* published a case series demonstrating the therapeutic potential of radiomicrospheres for various inoperable non-liver malignancies (*20*). ^{90}Y microspheres of size 40-60μm were used to treat 31 patients by various methods of microsphere placement. Of these, 7 patients underwent intra-arterial injection of ^{90}Y microspheres to treat tumors in the lung (pulmonary artery), stomach (right gastric artery), leg (superficial femoral artery) and tongue (lingual artery). Despite significant adverse events, objective clinical response was seen in 3 patients, including complete tumor regression for a case of metastatic squamous cell carcinoma to the popliteal fossa (*20*). More recently, MacKie *et al.* demonstrated in healthy porcine kidneys that super-selective ^{90}Y radioembolization can achieve targeted renal parenchymal destruction (*21*). A phase I clinical trial using ^{90}Y radioembolization to treat renal cell carcinoma is currently underway in Australia (*22*).

8. PATIENT 3 SUPPLEMENTAL TEXT

Patient 3 had multiple medical co-morbidities including Stage 5 chronic kidney disease on hemodialysis and recurrent gross hematuria due to severe radiation cystitis from EBRT for a previous gynecological malignancy. The HCC (BCLC D) was a new incidental finding during urological imaging. Following a multi-disciplinary medical and family conference, the patient received ^{90}Y radioembolization while undergoing acute in-patient urological treatment for gross hematuria. Her in-patient course was stormy and she died 5 weeks post-radioembolization due to sepsis and uro-surgical complications unrelated to ^{90}Y radioembolization.

REFERENCES

(1) Kao YH, EH Tan, CE Ng, SW Goh. State-of-the-art yttrium-90 selective internal radiation therapy: technical aspects of artery-specific SPECT/CT partition model dosimetry [abstract]. *J Nucl Med.* 2011;52(Suppl 1):1084.

(2) Kao YH, Tan EH, Ng CE, Goh SW. Artery-specific SPECT/CT partition model dosimetry. http://www.sgh.com.sg/clinical-departments-centers/nuclear-medicine-pet/pages/artery-specificspectctpartitionmodeldosimetry.aspx. *Department of Nuclear Medicine and PET, Singapore General Hospital, Singapore*. June 2011.

(3) Salem R, Thurston KG. Radioembolization with 90yttrium microspheres: a state-of-the-art brachytherapy treatment for primary and secondary liver malignancies. Part 1: technical and methodologic considerations. *J Vasc Interv Radiol*. 2006;17:1251-1278.

(4) Kennedy A, Nag S, Salem R, et al. Recommendations for radioembolization of hepatic malignancies using yttrium-90 microsphere brachytherapy: a consensus panel report from the radioembolization brachytherapy oncology consortium. *Int J Radiat Oncol Biol Phys*. 2007;68:13-23.

(5) Garin E, Rolland Y, Lenoir L, et al. Utility of quantitative Tc-MAA SPECT/CT for yttrium-labelled microsphere treatment planning: calculating vascularized hepatic volume and dosimetric approach. *Int J Mol Imaging*. July 28, 2011 [Epub ahead of print].

(6) Cremonesi M, Ferrari M, Bartolomei M. Radioembolisation with 90Y-microspheres: dosimetric and radiobiological investigation for multi-cycle treatment. *Eur J Nucl Med Mol Imaging*. 2008;35:2088-2096.

(7) Kennedy A, Dezarn W, Weiss A. Patient specific 3D image-based radiation dose estimates for 90Y microsphere hepatic radioembolization in metastatic tumors. *J Nucl Med Radiat Ther*. 2011;2:1-8.

(8) Kao YH, Tan EH, Teo TK, Ng CE, Goh SW. Imaging discordance between hepatic angiography versus Tc-99m-MAA SPECT/CT: a case series, technical discussion and clinical implications. *Ann Nucl Med*. July 16, 2011 [Epub ahead of print].

(9) Mallinckrodt Medical BV, LE Petten, Holland. *Technescan LyoMAA package insert*. June 28, 2007.

(10) Burton MA, Gray BN, Klemp PF, Kelleher DK, Hardy N. Selective internal radiation therapy: distribution of radiation in the liver. *Eur J Cancer Clin Oncol*. 1989;25:1487-1491.

(11) Fox RA, Klemp PF, Egan G, Mina LL, Burton MA, Gray BN. Dose distribution following selective internal radiation therapy. *Int J Radiat Oncol Biol Phys*. 1991;21:463-467.

(12) Lau WY, Leung TW, Ho S, et al. Diagnostic pharmaco-scintigraphy with hepatic intra-arterial technetium-99m macroaggregated albumin in the determination of tumour to non-tumour uptake ratio in hepatocellular carcinoma. *Br J Radiol*. 1994;67:136-139.

(13) Ho S, Lau WY, Leung TW, et al. Tumor-to-normal uptake ratio of 90Y microspheres in hepatic cancer assessed with 99Tcm macroaggregated albumin. *Br J Radiol*. 1997;70:823-828.

(14) Ho S, Lau WY, Leung TW, Chan M, Johnson PJ, Li AK. Clinical evaluation of the partition model for estimating radiation doses from yttrium-90 microspheres in the treatment of hepatic cancer. *Eur J Nucl Med.* 1997;24:293-298.

(15) Flamen P, Vanderlinden B, Delatte P, et al. Multimodality imaging can predict the metabolic response of unresectable colorectal liver metastases to radioembolization therapy with yttrium-90 labeled resin microspheres. *Phys Med Biol*. 2008;53:6591-6603.

(16) Leung WT, Lau WY, Ho SK, et al. Measuring lung shunting in hepatocellular carcinoma with intrahepatic-arterial technetium-99m macroaggregated albumin. *J Nucl Med.* 1994;35:70-73.

(17) Pereira JM, Stabin MG, Lima FR, Guimarães MI, Forrester JW. Image quantification for radiation dose calculations - limitations and uncertainties. *Health Phys*. 2010;99:688-701.

(18) Kawakami Y, Suga K, Yamashita T, Iwanaga H, Zaki M, Matsunaga N. Initial application of respiratory-gated 201Tl SPECT in pulmonary malignant tumours. *Nucl Med Commun*. 2005;26:303-313.

(19) Willowson K, Bailey DL, Baldock C. Quantifying lung shunting during planning for radio-embolization. *Phys Med Biol*. 2011;56:145-152.

(20) Blanchard RJ, Lafave JW, Kim YS, Frye CS, Ritchie WP, Perry JF Jr. Treatment of patients with advanced cancer utilizing Y90 microspheres. *Cancer*. 1965;18:375-380.

(21) Mackie S, de Silva S, Aslan P, et al. Super selective radio embolization of the porcine kidney with (90)yttrium resin microspheres: a feasibility, safety and dose ranging study. *J Urol*. 2011;185:285-290.

(22) Sirtex Technology Pty Ltd, New South Wales, Australia. Pilot study of Selective Internal Radiation Therapy (SIRT) with yttrium-90 resin microspheres (SIR-Spheres microspheres) in patients with renal cell carcinoma (STX0110, 'RESIRT'). *Australiancancertrials.gov.au*. September 15, 2010.

SUPPLEMENTAL FIGURE 1

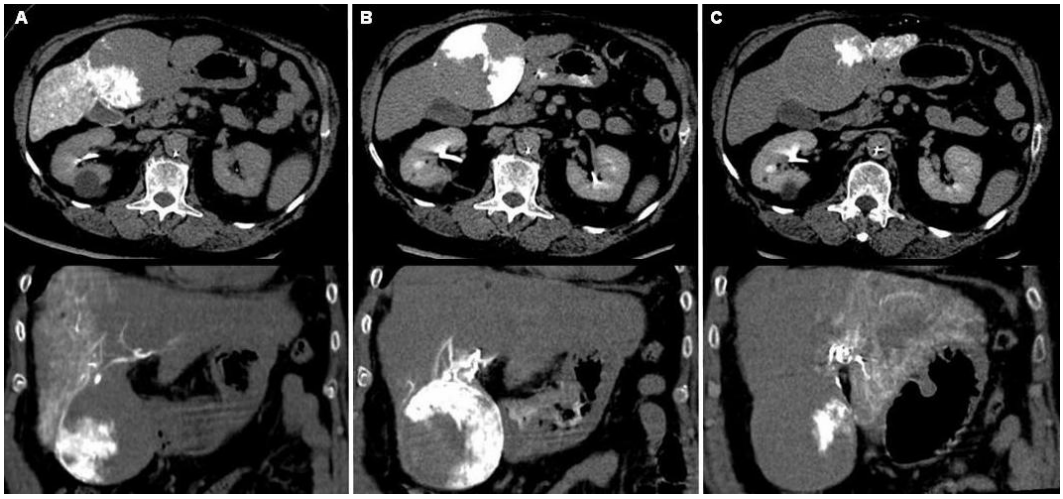

An example to illustrate the superior capability of catheter-directed CT hepatic angiography (CTHA) in delineating arterial territorial margins. Images depict catheter-directed CTHA obtained in the right (A), middle (B) and left (C) hepatic arteries in transaxial and coronal views respectively. It shows an exophytic HCC in segment IVb supplied by all three arteries with distinct territorial boundaries. Such tumors are suitable for sub-lesional dosimetry by artery-specific SPECT/CT partition modeling.

SUPPLEMENTAL FIGURE 2

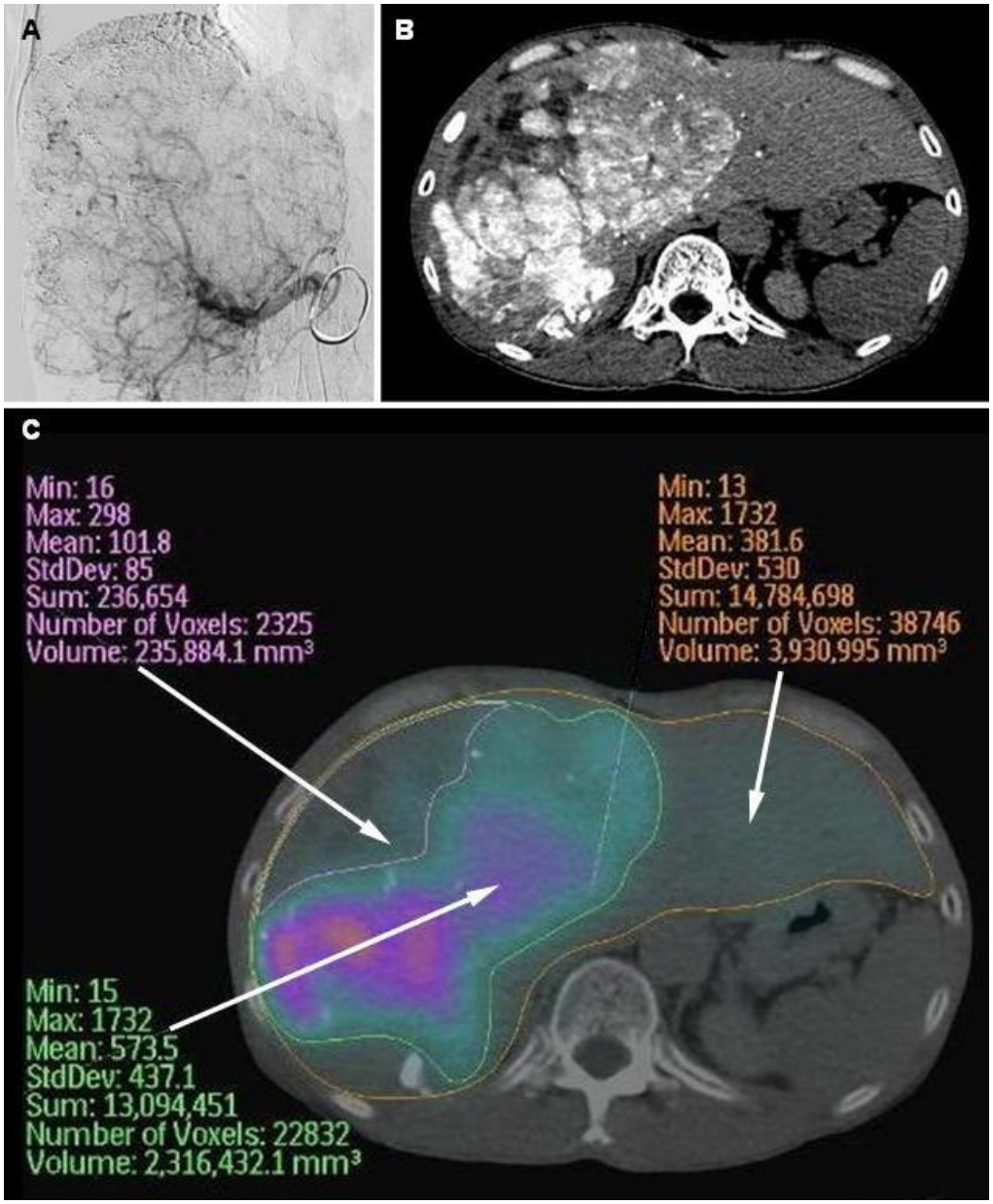

An example of artery-specific SPECT/CT partition modeling of a single arterial territory. Digital subtraction angiogram with catheter tip at the proper hepatic artery shows a single large hypervascular tumor (A). Corresponding catheter-directed CTHA shows the large contrast-enhancing tumor and delineates the planning target volume (B). Regions-of-interest (ROI) are drawn on ^{99m}Tc-MAA SPECT/CT (C) transaxial slices representing implanted tumor (green ROI), necrotic tumor (pink ROI) and the planning target volume (orange ROI).

SUPPLEMENTAL FIGURE 3

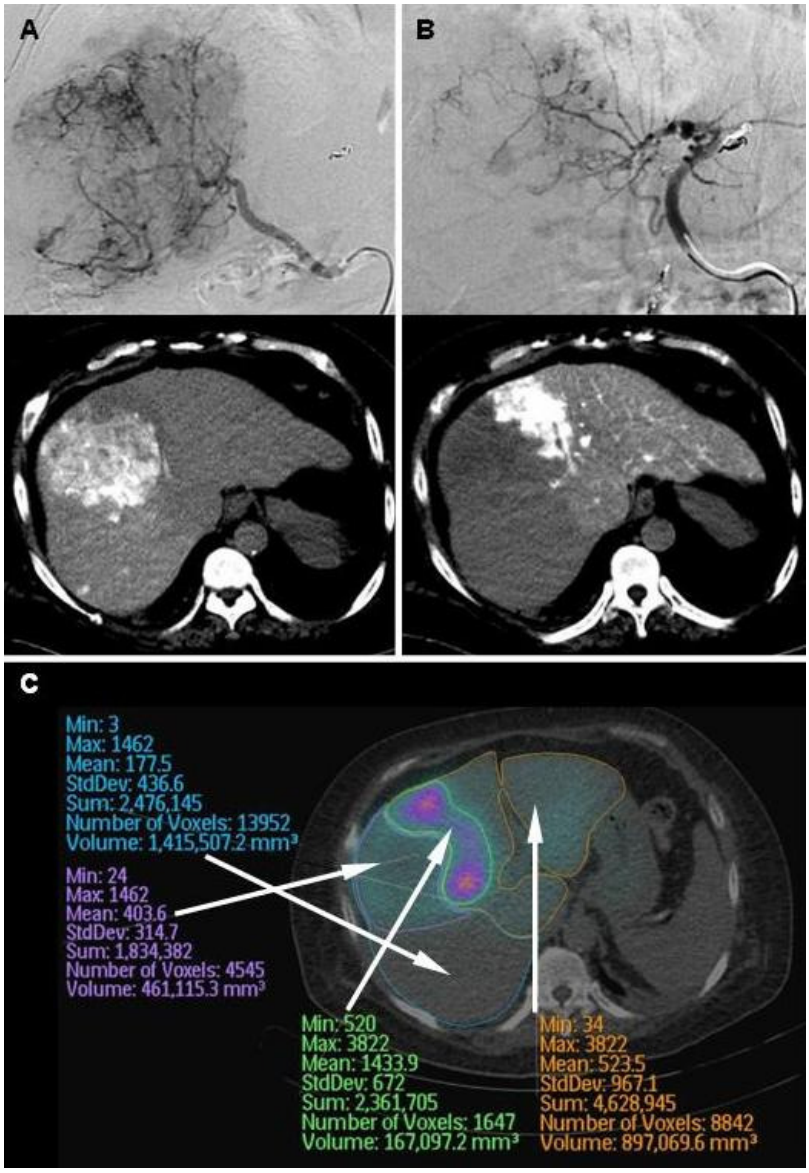

Patient 3: Example of sub-lesional artery-specific SPECT/CT partition modeling in two arterial territories. A single large HCC is supplied by both right (A) and left (B) hepatic arteries, depicted here in digital subtraction angiography and catheter-directed CTHA respectively. Regions-of-interest (ROI) drawn on ^{99m}Tc-MAA SPECT/CT are in keeping with planning target volumes delineated by catheter-directed CTHA. Blue ROI: right hepatic artery planning target volume; purple ROI: lateral half of the tumor supplied by right hepatic artery; orange ROI: left hepatic artery planning target volume; green ROI: medial half of the tumor supplied by the left hepatic artery. Each of the two halves of the tumor has an independent dosimetric plan i.e. 'sub-lesional' dosimetry.

SUPPLEMENTAL FIGURE 4

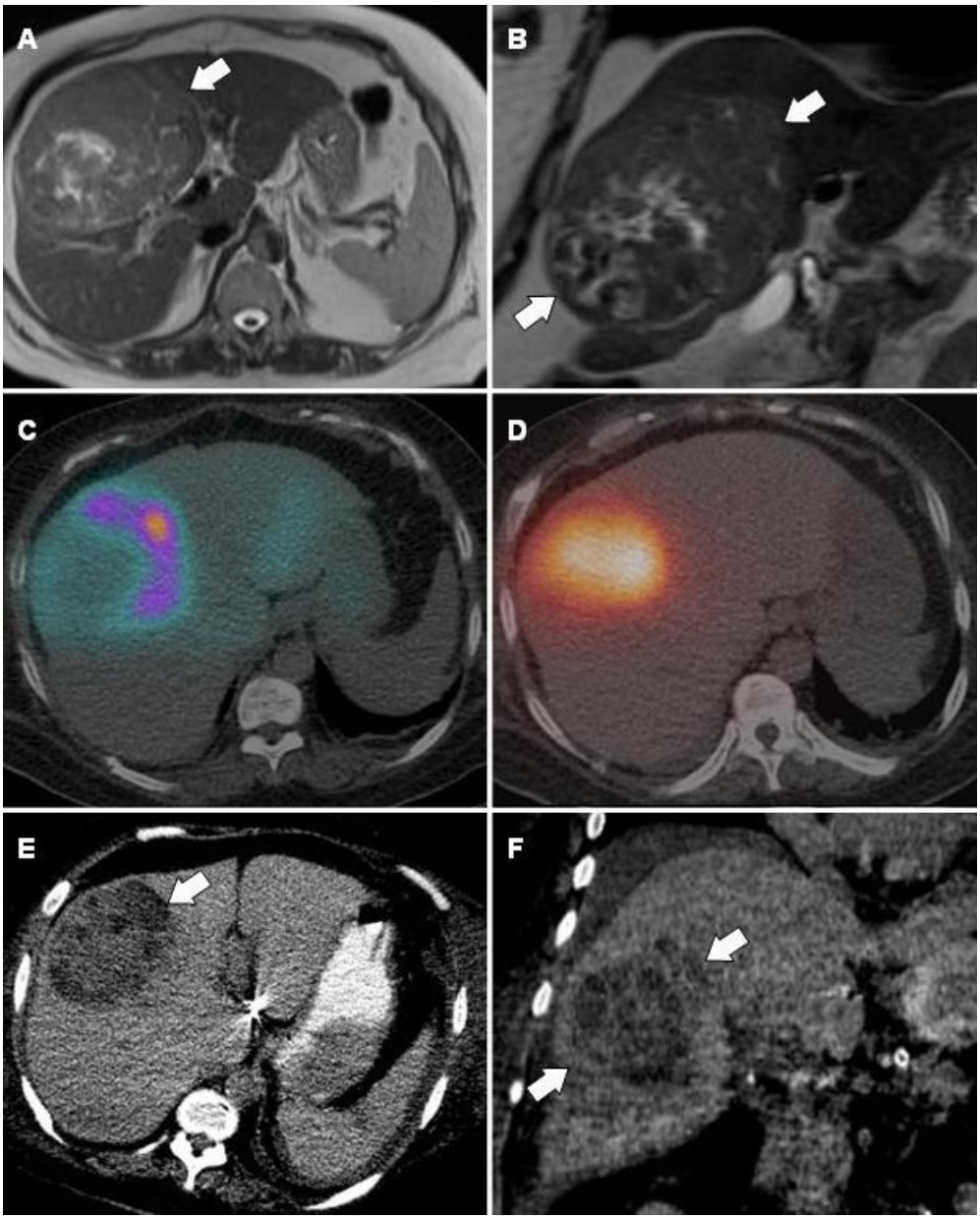

Patient 3: Example of clinically successful sub-lesional dosimetry. T2-weighted MRI liver shows a large central HCC (A transaxial; B coronal). Sub-lesional dosimetry was performed by regions-of-interest (ROI) contouring on ^{99m}Tc-MAA SPECT/CT based on arterial territories (C; Supplemental Fig. 3). Post-radioembolization bremsstrahlung SPECT/CT showed good tumoral activity, indicating technical success (D). Non-contrast enhanced CT abdomen 4 weeks post-embolization showed interval tumor regression (E transaxial; F coronal), indicating clinical success.

SUPPLEMENTAL FIGURE 5

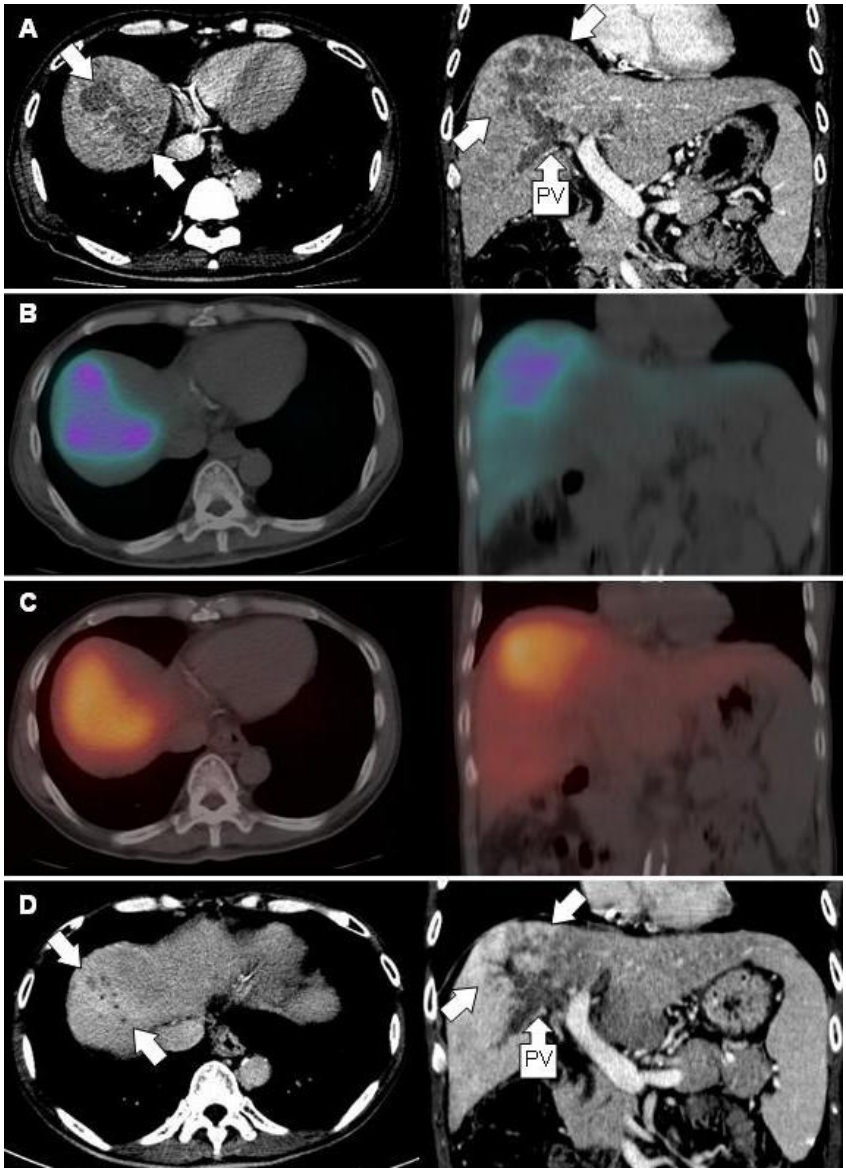

Patient 1: Example of clinical failure. Triphasic CT liver (portovenous phase) shows an infiltrative HCC (A, arrow) in segment VIII with branch portal vein tumor thrombosis (A, 'PV'). ^{99m}Tc-MAA SPECT/CT shows good segment VIII tumoral implantation (B). Post-radioembolization bremsstrahlung SPECT/CT shows good tumoral activity in segment VIII (C). However, technical success was 'indeterminate' due to ill-defined tumor margins, below bremsstrahlung SPECT/CT spatial resolution. Triphasic CT liver (portovenous phase) 8 weeks post-radioembolization showed interval regression of the segment VIII tumor (D, arrow), but progression of the branch portal vein tumor thrombosis (D, 'PV'), indicating clinical failure.

SUPPLEMENTAL TABLE 1: Patient characteristics

Patient No.	Age	Sex	Tumor	Risk factor	Previous Treatment	ECOG	Child-Pugh
1	58	M	HCC	HCV	Segmentectomy; sorafenib	1-2	A
2	63	M	HCC	HBV	Y-90 RE; segmentectomy	0	A
3	61	F	HCC	Cryptogenic	No	3	A
4	48	M	HCC	HBV	RFA	1-2	B
5	60	M	HCC	Cryptogenic	No	0	A
6	56	M	HCC	HBV	Right hemi-hepatectomy; TACE	0	A
7	61	F	HCC	Cryptogenic	Y-90 RE	1-2	A
8	65	M	HCC	HCV	No	0	B
9	56	M	HCC	HBV	No	0	A
10	52	M	HCC	HCV	No	0	A

HCC: hepatocellular carcinoma; HBV: chronic hepatitis B; HCV: chronic hepatitis C; ECOG: Eastern cooperative oncology group performance status; PV: portal vein; Y-90 RE: ^{90}Y radioembolization; RFA: radiofrequency ablation; TACE: transarterial chemoembolization

SUPPLEMENTAL TABLE 2: Disease characteristics

Patient No.	UNOS T-stage	BCLC	Tumor extent	Vascular invasion	Site of hepatic intra-arterial ^{99m}Tc-MAA injection
1	T4b	C	Bilobar; infiltrative	Branch PV	Right; left *
2	rT2	A	Solitary recurrence at segment IV resection margin	No	Right; left *
3	T3	D	Central large dominant tumor; smaller satellite lesions	No	Right; left *
4	T4b	C	Right lobe; multifocal	Branch PV	Superior branch of right; posterior branch of right †
5	T4b	C	Bilobar; multifocal; subcentimeter lesions present	Branch PV	Right; accessory right; left *
6	T4b	B	Bilobar; multifocal; subcentimeter lesions present	No	Right; left *
7	T4a	B	Right lobe; large necrotic tumor; satellite lesions with ill-defined margins	No	Right; middle †
8	T4a	B	Bilobar; multifocal; subcentimeter lesions present	No	Right; middle; left *
9	T4b	C	Bilobar; multifocal; subcentimeter lesions present	Branch PV	Proper *
10	T4b	C	Large right lobe tumor with ill-defined margins; subcentimeter lesion present	Branch and main PV; right hepatic vein	Right †

UNOS: United Network for Organ Sharing staging system, all patients are N0 M0; BCLC: Barcelona Clinic Liver Cancer staging system; PV: portal vein; * Whole-liver ^{99m}Tc-MAA injection; † Selective lobar/segmental ^{99m}Tc-MAA injection

SUPPLEMENTAL TABLE 3: Biochemical changes within 24 hours post-radioembolization

Patient No.	Baseline bilirubin (μmol/L)	24h post-RE bilirubin (μmol/L)	Baseline albumin (g/L)	24h post-RE albumin (g/L)	Baseline ALT (U/L)	24h post-RE ALT (U/L)	Baseline PT (sec)
1	30 CTCAE 1	Not done	28 CTCAE 2	Not done	33 CTCAE 0	Not done	11.3 CTCAE 1
2	20 CTCAE 0	32 CTCAE 1	37 CTCAE 0	37 CTCAE 0	29 CTCAE 0	44 CTCAE 1	10.3 CTCAE 0
3	27 CTCAE 1	19 CTCAE 0	19 CTCAE 3	19 CTCAE 3	51 CTCAE 1	44 CTCAE 1	10.2 CTCAE 0
4	25 CTCAE 1	36 CTCAE 1	25 CTCAE 2	26 CTCAE 2	19 CTCAE 0	22 CTCAE 0	12.2 CTCAE 1
5	18 CTCAE 0	13 CTCAE 0	37 CTCAE 0	31 CTCAE 0	44 CTCAE 1	41 CTCAE 1	10.2 CTCAE 0
6	20 CTCAE 0	18 CTCAE 0	29 CTCAE 2	25 CTCAE 2	56 CTCAE 1	42 CTCAE 1	10.8 CTCAE 0
7	26 CTCAE 1	26 CTCAE 0	29 CTCAE 2	29 CTCAE 2	30 CTCAE 0	31 CTCAE 0	11.9 CTCAE 1
8	44 CTCAE 2	35 CTCAE 1	22 CTCAE 2	21 CTCAE 2	59 CTCAE 1	51 CTCAE 1	12.8 CTCAE 1
9	26 CTCAE 1	Not done	35 CTCAE 1	Not done	122 CTCAE 2	Not done	11.3 CTCAE 1
10	15 CTCAE 0	17 CTCAE 0	34 CTCAE 1	33 CTCAE 1	22 CTCAE 0	21 CTCAE 0	10.9 CTCAE 0

RE: ^{90}Y radioembolization; ALT: alanine transaminase; PT: prothrombin time; CTCAE: Common Terminology Criteria for Adverse Events v4.03; Normal reference ranges: bilirubin 3-24 μmol/L; albumin 37-51 g/L; ALT 7-36 U/L; PT 9.2-11.2 sec

SUPPLEMENTAL TABLE 4: Greatest change in biochemistry within 3 months post-radioembolization

Patient No.	Days post-RE	Post-RE bilirubin (μmol/L)	Post-RE albumin (g/L)	Post-RE PT (sec)	Post-RE ALT (U/L)
1	89	53 CTCAE 2	20 CTCAE 2	13.9 CTCAE 1	52 CTCAE 1
2	34	22 CTCAE 0	33 CTCAE 2	10.7 CTCAE 0	72 CTCAE 1
5	80	44 CTCAE 2	35 CTCAE 2	10.3 CTCAE 0	105 CTCAE 1
6	100	20 CTCAE 0	36 CTCAE 1	Not done	40 CTCAE 1
7	66	61 CTCAE 2	26 CTCAE 2	13.4 CTCAE 1	30 CTCAE 0
9	15	23 CTCAE 0	36 CTCAE 1	Not done	81 CTCAE 1
10	62	14 CTCAE 0	31 CTCAE 1	Not done	32 CTCAE 0

RE: ^{90}Y radioembolization; ALT: alanine transaminase; PT: prothrombin time; CTCAE: Common Terminology Criteria for Adverse Events v4.03; Normal reference ranges: bilirubin 3-24 μmol/L; albumin 37-51 g/L; ALT 7-36 U/L; PT 9.2-11.2 sec

SUPPLEMENTAL TABLE 5: Best post-radioembolization alphafetoprotein response

Patient No.	Days post-RE	Baseline AFP (μg/L)	Best post-RE AFP (μg/L) (% change)
1	44	3,412	428 (-87%)
2	80	6,353	313 (-95%)
5	120	>60,500	41,220 (> -32%)
6	89	Not elevated	Not elevated
7	118	Not elevated	Not elevated

RE: ^{90}Y radioembolization; AFP: serum alphafetoprotein; Normal reference range: serum alphafetoprotein <7.1 μg/L

SUPPLEMENTAL TABLE 6: Best post-radioembolization imaging response

Pt No.	Days post-RE	Pre-RE index lesion (cm)	Post-RE index lesion (cm); (% change)*	New lesions within PTV	Tumor vascular involvement	Clinical success	New extra-hepatic metastasis	RECIST	WHO	EASL
1	62	9.1 x 7.1	3.7 x 1.9 (-89%)	No	Progression	No	No	PD	PD	PD
2	157	4.2 x 3.2	1.9 x 1.7 (-76%)	No	No	Yes	Lung	PD	PD	PD
3	29	12.2 x 9.9	8.6 x 6.7 (-52%)	No	No	Yes	No	PR	PR	PR
5	108	12.3 x 10.5	10.0 x 8.5 (-34%)	No	Stable	Yes	Adrenal	PD	PD	PD
6	121	3.0 x 2.5	2.4 x 2.0 (-36%)	No	No	Yes	Lung	PD	PD	PD
7	89	10.7 x 9.7	10.2 x 7.6 (-25%)	No	No	Yes	No	SD	SD	SD
9	48	13.5 x 9.0	8.1 x 5.5 (-63%)	No	Regression	Yes	No	PR	PR	PR
10	62	11.0 x 10.0	5.4 x 5.0 (-75%)	No	Regression	Yes	No	PR	PR	PR

RE: ^{90}Y radioembolization; * Difference in cross-product; PTV: planning target volume; RECIST: Response Evaluation Criteria in Solid Tumors version 1.1; WHO: World Health Organization guidelines for imaging response; EASL: 2-D European Association for the Study of the Liver (2D-EASL) guidelines for imaging response

SUPPLEMENTAL TABLE 7: Imaging time-to-progression and overall survival

Patient No.	Multimodality therapy †	Imaging time-to-progression within planning target volumes	Survival from diagnosis	Survival from Y-90 RE
1	Yes	8wk (2mth) ‡	95wk (22mth)	13wk (3mth)
2*	Yes	>29wk (7mth) §	>71wk (16mth)	>67wk (15mth)
5	Yes	>21wk (5mth)	>33wk (8mth)	>21wk (5mth)
6	Yes	>21wk (5mth)	>91wk (21mth)	>21wk (5mth)
7*	No	>17wk (4mth) §	>71wk (16mth)	>68wk (16mth)
9	No	>12wk (3mth)	>21wk (5mth)	>12wk (3mth)
10	No	>12wk (3mth)	>17wk (4mth)	>12wk (3mth)

* Survival from first ^{90}Y radioembolization; † Multimodality therapy refers to any combination of systemic chemotherapy, transarterial chemoembolization (TACE), or local ablative techniques at any stage of the disease; ‡ Infiltrative HCC with progression of existing portal vein tumor thrombosis despite significant reduction in index tumor size; § Calculated from second ^{90}Y radioembolization

SUPPLEMENTAL TABLE 8: Summary of required dosimetric variables

1. Perfused territory SPECT/CT VOI (mm^3)
2. Perfused territory SPECT/CT VOI counts
3. Implanted tumor SPECT/CT VOI (mm^3)
4. Implanted tumor SPECT/CT counts
5. Implanted tumor mean SPECT/CT count density (counts/mm^3)
6. Implanted non-tumorous liver SPECT/CT VOI (mm^3)
7. Implanted non-tumorous liver SPECT/CT counts
8. Implanted non-tumorous liver mean SPECT/CT count density (counts/mm^3)
9. SPECT/CT-based artery-specific mean T/N ratio

VOI: volume of interest; T/N: tumor-to-normal liver

SUPPLEMENTAL TABLE 9: Items to be excluded from dosimetric analyses

1. Non-functioning non-tumorous liver, e.g.:
    a. Liver cysts;
    b. Post-radiofrequency ablation cavities
2. Liver tumors detected on diagnostic imaging, but do not exhibit significant focal ^{99m}Tc-MAA activity on SPECT/CT, e.g.:
    a. Regions of necrotic tumor;
    b. Hypovascular tumors - unless intended for radioembolization segmentectomy/lobectomy

TABLE 10
Dosimetric Data by Artery-Specific SPECT/CT Partition Modeling

Patient no.	First ^{90}Y-RE radiation dose	Planning target volume 1	Planning target volume 2	Planning target volume 3	Artery prophylactic coil embolization	Liver–lung shunt	Total injected ^{90}Y activity	Technical success*
1	NA	Right hepatic artery	Left hepatic artery	NA	No	8.3% (5 Gy)	2.1 GBq	Indeterminate; ill-defined tumor margins†
		T/N ratio, 5.7	T/N ratio, 8.1					
		Tumor mass, 259 g	Tumor mass, 46 g					
		Tumor dose, 171 Gy	Tumor dose, 177 Gy					
		Liver mass, 920 g	Liver mass, 833 g					
		Liver dose, 30 Gy	Liver dose, 22 Gy					
		^{90}Y activity, 1.6 GBq	^{90}Y activity, 0.5 GBq					
2	Liver, 70 Gy; lung, 9 Gy‡	Right hepatic artery	Left hepatic artery§	NA	No	4.5% (1 Gy)	1.0 GBq	Yes
		T/N ratio, 6.1	T/N ratio, 1.4					
		Tumor mass, 7 g	Tumor mass, 28 g					
		Tumor dose, 164 Gy	Tumor dose, 133 Gy					
		Liver mass, 782 g	Liver mass, 256 g					
		Liver dose, 27 Gy	Liver dose, 93 Gy					
		^{90}Y activity, 0.4GBq	^{90}Y activity, 0.6 GBq					
3	NA	Right hepatic artery	Left hepatic artery	NA	Accessory left gastric; gastroduodenal‖	4.6% (2 Gy)	1.4 GBq	Indeterminate; subcentimeter lesions¶
		T/N ratio, 6.5	T/N ratio, 4.6					
		Tumor mass, 410 g	Tumor mass, 172 g					
		Tumor dose, 92 Gy	Tumor dose, 59 Gy					
		Liver mass, 983 g	Liver mass, 752 g					
		Liver dose, 14 Gy	Liver dose, 13 Gy					
		^{90}Y activity, 1.0 GBq	^{90}Y activity, 0.4 GBq					
4	NA	Right hepatic artery (superior branch)	Right hepatic artery (posterior branch)	NA	No	10.3% (9 Gy)	2.6 GBq	Yes
		T/N ratio, 8.1	T/N ratio, 8.4					
		Tumor mass, 58 g	Tumor mass, 484 g					
		Tumor dose, 241 Gy	Tumor dose, 176 Gy					
		Liver mass, 189 g	Liver mass, 825 g					
		Liver dose, 30 Gy	Liver dose, 21 Gy					
		^{90}Y activity, 0.4 GBq	^{90}Y activity, 2.2 GBq					
5	NA	Right hepatic artery	Accessory right hepatic artery	Left hepatic artery	No	3.5% (2 Gy)	3.2 GBq	Indeterminate; subcentimeter lesions¶
		T/N ratio, 5.2	T/N ratio, 3.1	T/N ratio, 2.3				
		Tumor mass, 337 g	Tumor mass, 730 g	Tumor mass, 12 g				
		Tumor dose, 135 Gy	Tumor dose, 87 Gy	Tumor dose, 106 Gy				
		Liver mass, 247 g	Liver mass, 423 g	Liver mass, 595 g				
		Liver dose, 26 Gy	Liver dose, 28 Gy	Liver dose, 47 Gy				
		^{90}Y activity, 1.1 GBq	^{90}Y activity, 1.5 GBq	^{90}Y activity, 0.6 GBq				
6	NA	Right hepatic artery	Left hepatic artery	NA	No	8.4% (2 Gy)	1.0 GBq	Indeterminate; subcentimeter lesions¶
		T/N ratio, 5.6	T/N ratio, 7.6					
		Tumor mass, 27 g	Tumor mass, 40 g					
		Tumor dose, 151 Gy	Tumor dose, 152 Gy					

TABLE 10 (Continued)

Patient no.	First ^{90}Y-RE radiation dose	Planning target volume 1	Planning target volume 2	Planning target volume 3	Artery prophylactic coil embolization	Liver–lung shunt	Total injected ^{90}Y activity	Technical success*
		Liver mass, 460 g	Liver mass, 1,196 g					
		Liver dose, 27 Gy	Liver dose, 20 Gy					
		^{90}Y activity, 0.4 GBq	^{90}Y activity, 0.6 GBq					
7	Liver, 40 Gy; lung, 10 Gy‡	Right hepatic artery	Middle hepatic artery	NA	Right inferior phrenic; falciform‖	4.3% (1 Gy)	1.0 GBq	Indeterminate; ill-defined tumor margins†
		T/N ratio, 2.1	T/N ratio, 1.7					
		Tumor mass, 156 g	Tumor mass, 12 g					
		Tumor dose, 106 Gy	Tumor dose, 85 Gy					
		Liver mass, 363 g	Liver mass, 252 g					
		Liver dose, 51 Gy	Liver dose, 51 Gy					
		^{90}Y activity, 0.7 GBq	^{90}Y activity, 0.3 GBq					
8	NA	Right hepatic artery	Left hepatic artery	Middle hepatic artery	Right gastric; gastroduodenal#	6.1% (3 Gy)	2.4 GBq	No; nonimplantation in caudate tumor
		T/N ratio, 2.4	T/N ratio, 4.3	T/N ratio, 3.2				
		Tumor mass, 266 g	Tumor mass, 23 g	Tumor mass, 10 g				
		Tumor dose, 91 Gy	Tumor dose, 107 Gy	Tumor dose, 95 Gy				
		Liver mass, 1,465 g	Liver mass, 1,044 g	Liver mass, 356 g				
		Liver dose, 38 Gy	Liver dose, 25 Gy	Liver dose, 30 Gy				
		^{90}Y activity, 1.6 GBq	^{90}Y activity, 0.6 GBq	^{90}Y activity, 0.2 GBq				
9	NA	Proper hepatic artery	NA	NA	Accessory left gastric‖; right gastric‖; gastroduodenal#; pancreaticoduodenal arcade#	1.7% (2 Gy)	2.6 GBq	Indeterminate; subcentimeter lesions¶
		T/N ratio, 11.5						
		Tumor mass, 1,252 g						
		Tumor dose, 97 Gy						
		Liver mass, 755 g						
		Liver dose, 8 Gy						
		^{90}Y activity, 2.6 GBq						
10	NA	Right hepatic artery	NA	NA	No	14.5% (16 Gy)	2.3 GBq	Indeterminate; ill-defined tumor margins; subcentimeter lesions†¶
		T/N ratio, 10.6						
		Tumor mass, 955 g						
		Tumor dose, 97 Gy						
		Liver mass, 350 g						
		Liver dose, 9 Gy						
		^{90}Y activity, 2.3 GBq						

RE = radioembolization; NA = not applicable; dose = predicted mean radiation absorbed dose in grays.

*As assessed by bremsstrahlung SPECT/CT.

†Ill-defined tumor margins that cannot be reliably assessed by bremsstrahlung SPECT/CT.

‡Planned by planar partition modeling.

§Planned by sublesional dosimetry with radiation lobectomy intent to left hepatic arterial territory.

‖Coil embolization at time of mapping hepatic angiography.

¶Subcentimeter lesions below bremsstrahlung SPECT/CT spatial resolution.

#Coil embolization at time of ^{90}Y radioembolization.